

## Suppression and Excitation of MHD Activity with Electrically Polarized Electrode at the TCABR Tokamak Plasma Edge

I. C. Nascimento 1), Yu. K. Kuznetsov 1), Z. O. Guimarães-Filho 1), I. El Chamaa-Neto 2), O. Usuriaga 1), A. M. M. Fonseca 1), R. M. O. Galvão 1, 4), I. L. Caldas 1), J. H. F. Severo 1), I. B. Semenov 3), M. V. P. Heller<sup>1</sup>, V. Bellintani 1), J. I. Elizondo 1) and E. Sanada 1)

1) Laboratório de Física de Plasmas, Instituto de Física, Universidade de São Paulo, São Paulo, Brasil

2) Universidade Tuiuti do Paraná, Curitiba, Brasil

3) Kurchatov Institute, Moscow, Russia

4) Centro Brasileiro de Pesquisas Físicas, Rio de Janeiro, Brasil

e-mail contact of main author: [inascime@if.usp.br](mailto:inascime@if.usp.br)

**Abstract.** Using a voltage biased electrode inside the edge of the tokamak TCABR, H-mode discharges with strong, Regime I, and partial or total suppressed MHD activity, Regime II, were obtained. In this paper we present the results of the study of these two regimes of operation. The experiment was carried out adjusting the tokamak parameters to obtain discharges with strong or weak MHD activity, without biasing in both cases. During the shots the plasma current varied to cover a range of safety factor from 2.8 up to 3.6, allowing the H-mode barrier to interact with the magnetic islands. Subsequently, the bias was applied and shots with and without MHD activity were obtained. An array of 22 Mirnov coils was used to detect the magnetic oscillations and a triple Langmuir probe to measure plasma floating potentials and ion saturation currents. The results show that the dominant modes are  $m=2$ ,  $n=1$  and  $m=3$ ,  $n=1$  for partial excitation and suppression, respectively. In both cases strong decrease of the radial electric field is detected with destruction of the transport barrier and of the H mode regime. The measurements include temporal behaviour of edge transport, turbulence, poloidal electric and magnetic fields, edge density, radial electric fields and radial profile of  $H_\alpha$  line intensity. The explanation of the excitation and suppression processes is discussed in the text.

### 1. Introduction

Among the main advances in tokamak research were the discovery of the H-mode in ASDEX in 1982 [1] and realization of the important role played by radial electric fields on plasma confinement, in particular for the control of turbulence. However, the influence of electric fields on MHD activity has not attracted much attention and, until recently, not very many papers have been published on this issue. In a previous paper we reported results of the insertion of an electrically polarized electrode at the edge of the tokamak TCABR showing discharges with increase of the confinement time by a factor up to 2 with small MHD oscillations, and others with strong MHD and confinement degradation [2]. Recently, similar results have been reported for the TUMAN-3M tokamak [3]. In reference [4] we investigated the influence of Mirnov oscillations on plasma transport and turbulence.

In this paper we report recent results of our investigation on MHD activity in experiments with the plasma in the H mode obtained using a voltage biased electrode inserted at the edge of the plasma column TCABR.

In section 2 we describe the experimental set-up, in section 3 the data is presented, analyzed and discussed and in section 4 we present the conclusions.

## 2. Experimental setup

The experiments were carried out on the TCABR tokamak, major radius  $R = 0.615$  m, minor radius  $a = 0.18$  m, toroidal field  $B_t = 1.07$  T, maximum plasma current  $I_{p, \max} = 110$  kA, circular cross-section shape, electron temperature  $T_e \sim 500$  eV. In this experimental campaign the density was adjusted at  $1.0 - 1.5 \times 10^{19} \text{ m}^{-3}$ , prior to application of the bias and, depending on the plasma conditions, could grow up to  $4.0 \times 10^{19} \text{ m}^{-3}$  with bias, and the plasma current from  $I_p = 83$  to 105 kA ( $q_a = 3.5$ -2.8). The movable electrode is of hard graphite 20 mm diameter and 8 mm thick disk fixed at the tip of a shaft insulated with an alumina tube. The front face of the electrode can be positioned, without disruptions, up to 2.0 cm into the plasma ( $r = 16.0$  cm), at the equatorial plane and low field side of the plasma column,  $160^\circ$  from the graphite limiter in the plasma current direction (counter-clockwise top view). The MHD activity is detected using a set of 22 Mirnov coils, circularly distributed in the poloidal direction at  $r=19.5$  cm (1.5 cm behind the limiter). A set of three electrostatic probes (triple probe) was used to measure the floating plasma potentials in two poloidal positions separated by 0.5 cm, and the ion saturation current at a toroidal position 0.5 cm apart from the poloidal probes. This triple probe can be moved from  $r = 21.0$  cm to 16.0 cm (2.0 inside the plasma to 3.0 cm behind the limiter). In this work the electrode front face position was placed at 17.0 cm or 16.5 cm, depending on the plasma parameters to avoid disruptions, and polarized positively in the voltage range from 300 to 400 V. The power supply can provide current and voltage up to 300 A and 750 V, respectively, with negative or positive polarities and is insulated from ground and from the power line. Using a triggered fast electronic switch and a large capacitor bank, pulses with rise time from 10  $\mu\text{s}$  to 10 ms can be obtained. The ion saturation current  $I_s$  and fluctuation potentials,  $V_{f1}$  and  $V_{f2}$ , at the edge and SOL were measured using the triple Langmuir probe. Radial profiles were obtained on shot-to-shot basis. Probe and Mirnov coil data were digitized at 1 megasample per second and filtered by a 300 kHz anti-aliasing filter. The intensity of the  $H_\alpha$  hydrogen spectral line was measured using 49 sensors viewing the plasma in two directions for tomography and Abel inversion.

## 3. Experimental data, analysis and discussion

To perform the experiments, the tokamak was configured to obtain discharges with central chord line-averaged densities of  $1.0 - 1.5 \times 10^{19} \text{ m}^{-3}$  with either strong or weak MHD activity before, the application of the bias. The plasma current was programmed to cover a range of safety factors  $q_a$  from 3.5 to 2.8, i.e.,  $I_p$  from 83 to 105 kA, allowing the  $q=3$  rational surface to be placed in the range between the electrode position at 16.5 or 17.0 cm and outside the plasma. The bias voltage duration was chosen to allow a density excursion up to the maximum value. The shots with the application of the bias were classified as Regime I and Regime II as indicated in figure. 1. Shots of Regime I do not show MHD activity without bias and usually show MHD with bias. Shots of Regime II show MHD activity without bias and total or partial suppression of MHD with bias. Typical discharges of the two types are shown in figure 1: (a) excitation and (b) partial and full suppression of MHD oscillations. Tests made with gas-puffing to obtain similar temporal evolution of the plasma density as that with biased electrode did not show equivalent results [2]. Therefore, we concluded that the effects described in this paper are caused by the influence of the electric field created by the electrode voltage.

For discharge 1, in figure 1(a) (Regime I), no bias was applied, the plasma current was 90 kA and  $q_a = 3.2$ . Assuming quasi-parabolic current distribution with exponent  $\alpha=2.4$ , for  $q = 3$

the rational surface is at  $r=17.3$  cm. As it can be observed the level of MHD activity is quite small. In shots 2 and 3, with the electrode biased at 350 V, and placed at  $r_E = 16.5$  cm, the figure shows MHD activity beginning in different instants of time and reaching high amplitudes. In shot 2 it begins to increase at 58 ms, reaches a maximum at 62 ms and then decays. In this time interval the rational surface for  $q=3$  moves from 17.6 to 17.3, a position coincident with that of the biased electrode, located at an average position  $r_E = 16.9 \pm 0.4$  cm (from 17.3 to 16.5 cm, thickness of 0.8 cm). The temporal evolution of the mode spectrum of the MHD instability, typical of the regime I, is shown in figure 2(a). For excitation with bias the dominant mode is (2, 1), ( $m=2$ ,  $n=1$ ), and mode (3, 1) is small as can be seen in the figure. Therefore, it seems that when the rational surface at  $q=3$  is close to the transport barrier, mode 3 is inhibited. The island (2, 1) located far from the electrode is not affected in this case.

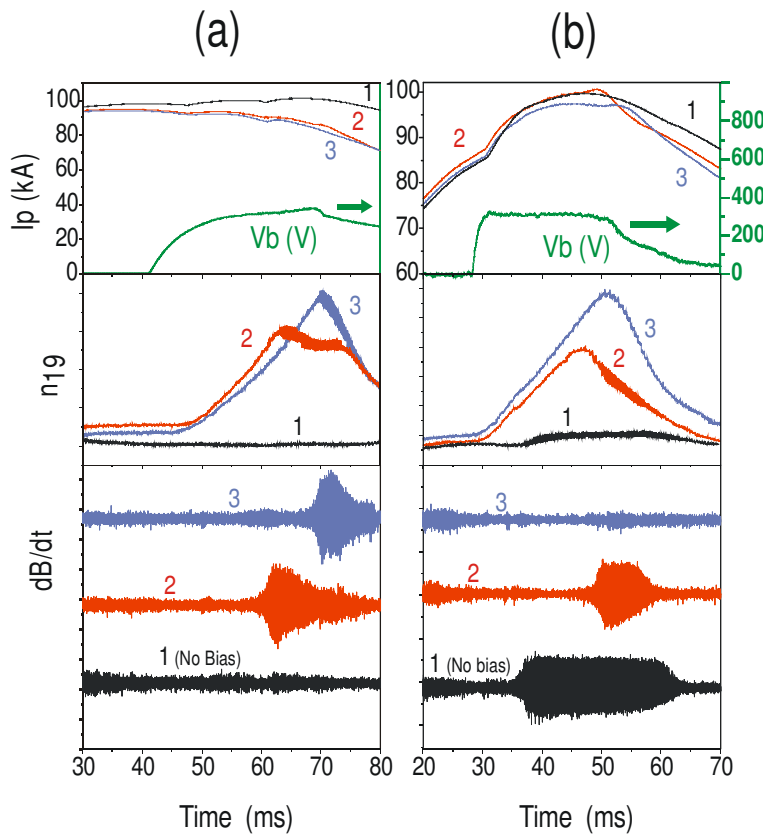


Figure 1: (a) – Regime I: Typical discharges with strong MHD activity during electrode biasing; (b) – Regime II: Typical discharges with partial or total suppression of high amplitude MHD activity.

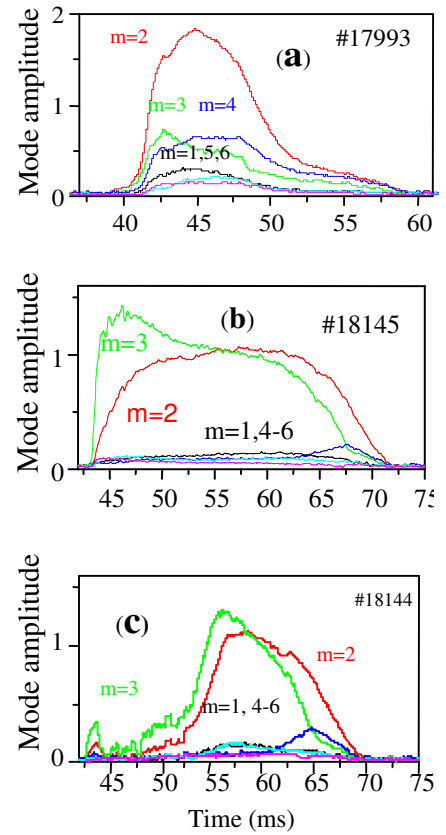


Figure 2. Time behaviour of MHD modes  $m = 2, 3, 4-6, n=1$ . (a) Shot #17993, Regime I, excitation with biasing; (b) Shot #18145, Regime II, without bias, with MHD; (c) Shot #18144 Regime II, partial suppression with bias

Now, let us examine discharges that show partial suppression (inhibition) of MHD activity with the application of the electrode voltage, in the regime II. In this scenario we start with discharges with high MHD activity before the application of the bias, figure 1(b), shot 1. Typical shots for this regime are presented in figure 1(b). Figures 2(b) and (c) show the temporal evolution of the MHD modes in the case of partial suppression without and with the application of the voltage bias, respectively. It can be seen that modes (3, 1) and (2, 1) have

large amplitudes and mode 3 is even substantially stronger at the beginning of instability. With the application of the bias, the instability is suppressed until about 50 ms and, then, both modes increase in amplitude.

Our qualitatively explanation of these facts is that mode (2, 1) is unstable (active) in regime I. In this case, the excitation of the relatively small (passive) mode (3, 1) results from the coupling with mode (2, 1) driven by toroidal effects. It seems that mode (3, 1) is active only in the regime II, at the beginning of the instability.

The effects of the electrode bias in regimes I (excitation of MHD activity) and II (partial suppression or weak MHD oscillations) on the transport of particles in the plasma edge and the plasma turbulence were studied using a triple probe to measure floating potentials and ion saturation currents. Mirnov coil, bolometer and diode arrays were used for measuring Mirnov oscillations, radiation emissions and the intensity of the  $H_\alpha$  line emission of hydrogen, respectively.

### 3.1 – Regime I – Bias excitation of MHD activity

In figures 3(a) to 3(d) we show for shot #17994 the data obtained using the diagnostics above mentioned. The effect of the electrode bias on the plasma transport and turbulence in regime I (excitation), with the electrode positioned at  $r_E = 16.5$  cm, (average position 16.9 cm), and the electrostatic triple probe at  $r_p = 17.0$  cm, are seen in figure 3(a). Triggering the electrode voltage bias, the average plasma density, measured at the central chord by the microwave interferometer increases, indicating improved global particle confinement. The root mean square of the poloidal electric field fluctuations  $E_{\theta, rms}$  decreases, the local average density  $n_{av}$ , measured by the probe increases, and the transport  $\Gamma$  decreases, indicating edge transport barrier formation. At the onset of MHD activity, indicated as the root mean square of the poloidal magnetic field fluctuations  $B_{\theta, rms}$ , the deterioration of the barrier is apparent, indicated by the increase of the transport, the decrease of the local density, the stop of the increase of the central chord line-averaged density which reaches a plateau, and the fast increase of the electrode current. After the decrease of MHD activity the density increases reaching a peak and again indicating particle confinement improvement. These results lead to the conclusion that plasma turbulence is suppressed by electrode bias but increases again with the growth of Mirnov oscillations. The time behaviour of the MHD mode spectrum is similar to shot #17993 shown in figure 2(a), where the (2, 1) is the dominant mode.

The radial electric field temporal behaviour at  $r = 17.5$  cm is shown in figure 3(c). It was obtained by measuring the floating potentials  $V_f$  in the region of influence of the electrode taking  $E_r \approx -\nabla V_f$ , (shots 17993/17994), and neglecting the influence of the temperature gradient. In small tokamaks like TCABR the influence of this gradient is usually within the error bars of the measurement. This measurement was based in two successive shots with good reproducibility. Nevertheless, even so, we estimated the influence of a hypothetical displacement of 1 ms between the shots to evaluate the reliability of the calculated electric field. The result is shown in the figure 3(c) with vertical error bars. As it can be seen the decrease of the electric field exists even with the displacement and the general behaviour remains the same. The comparison of the temporal behaviours of the radial electric field, figure 3(c), with the MHD activity, figure 3(b), shows that there is a decrease of the electric field near the onset of the MHD instability. After this it recovers slowly to the previous value as the MHD amplitude saturates. On the other hand, the electrode current  $I_b$  after reaching a

peak decays during the saturated MHD activity while the central chord density stays flat. In conclusion, at about 40 ms the plasma enters the H-mode type regime, but the onset of MHD activity destroys the barrier. This behaviour is expected theoretically according to Stringer's neoclassical calculations of transport with impurities taking into account non-ambipolarity in the presence of electrostatic and magnetic fluctuations [5]. With the confinement improvement, impurities accumulate in the plasma central region increasing radiation losses, and leading to strong MHD activity. The resulting cooling can be seen in the loop voltage (not shown here) which increases about 0.6 V peak (25%). With the overlapping of the magnetic islands and the stochasticization of the magnetic field a large parallel electron flux can strongly influence the radial electric field. The strong effect of the MHD oscillations can be inferred from the  $H_\alpha$  not normalized line intensity radial profile represented in figure 3(d) by blue triangles, compared to the red circles for H mode and black squares L mode. In this case the excited MHD activity is responsible for the destruction of the barrier and the H mode.

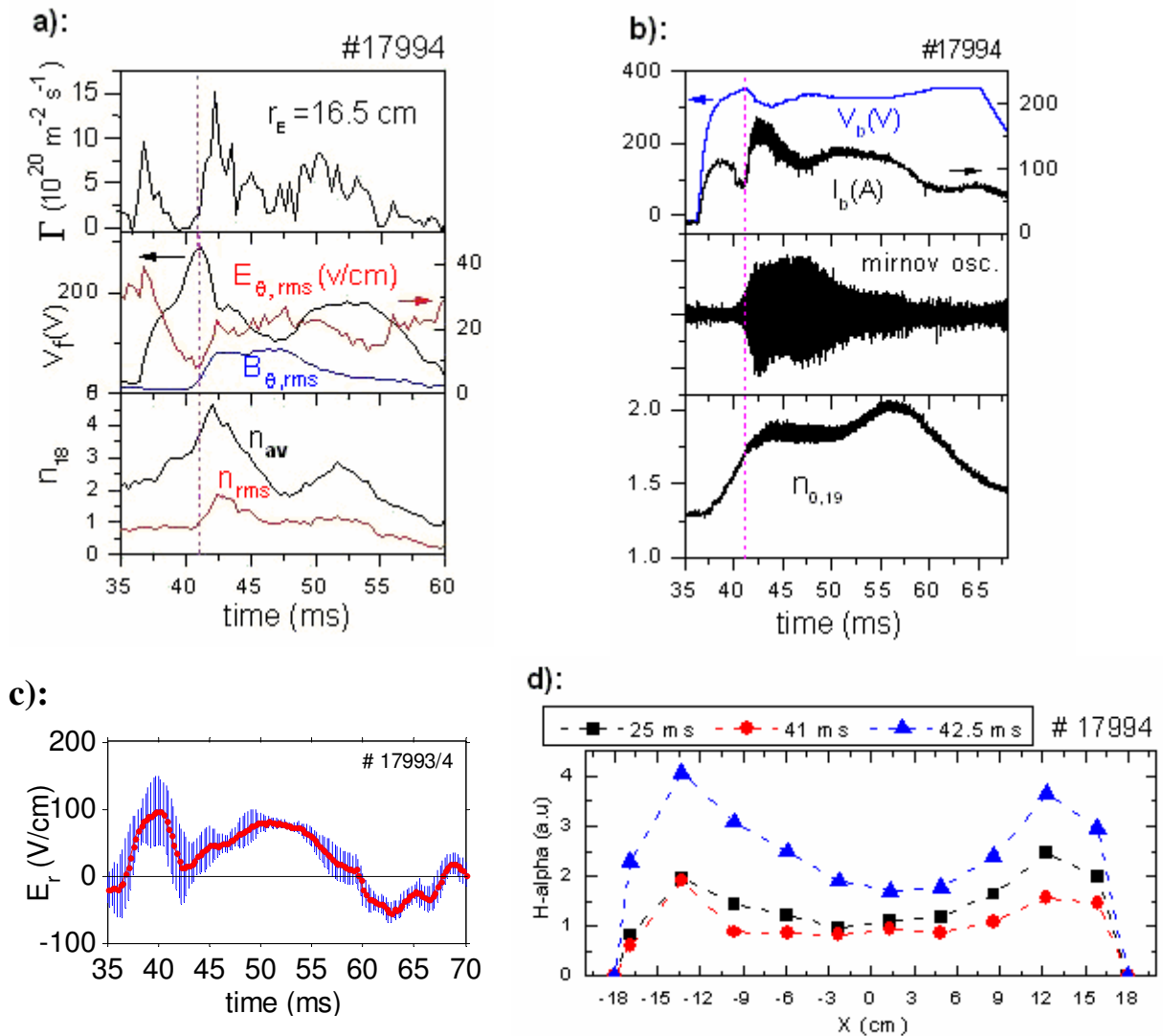


Figure 3. Effect of electrode voltage on edge plasma parameters. Plasma in regime I with electrode at  $r_E = 16.5$  cm, for shot #17994. Temporal behaviour at  $r = 17.0$  cm of: (a) transport, floating potential, root mean square of the poloidal electric and magnetic field fluctuations  $E_{\theta, \text{rms}}$ ,  $B_{\theta, \text{rms}}$ , respectively; (b) voltage and electrode current, Mirnov oscillations, dB/dt, and central chord line-averaged current; (c) electric field at  $r = 17.5$  cm. (d) Radial profile of the  $H_\alpha$  emission at 28 ms, before biasing, 41 ms and 42.5 ms with biasing and without and with MHD activity, respectively.

### 3.2 – Regime II – Bias suppression of MHD activity

In figure 4 (a) to 4(d) we present experimental results of the study of the partial suppression of the MHD activity in regime II for shot #18696, similar to shot 18144 of figure 2(c). The electrode front face was positioned at  $r_E = 17.0$  cm and the triple probe also at 17.0 cm. The figures show clearly that the plasma entered the H-mode at 35 ms, evidenced by the fast decrease of plasma transport, poloidal electric field fluctuations,  $E_{\theta,rms}$ , ion saturation current fluctuations,  $n_{rms}$ , and decrease of the  $H_\alpha$  intensity throughout the radial profile shown as red circles in figure 4(d).

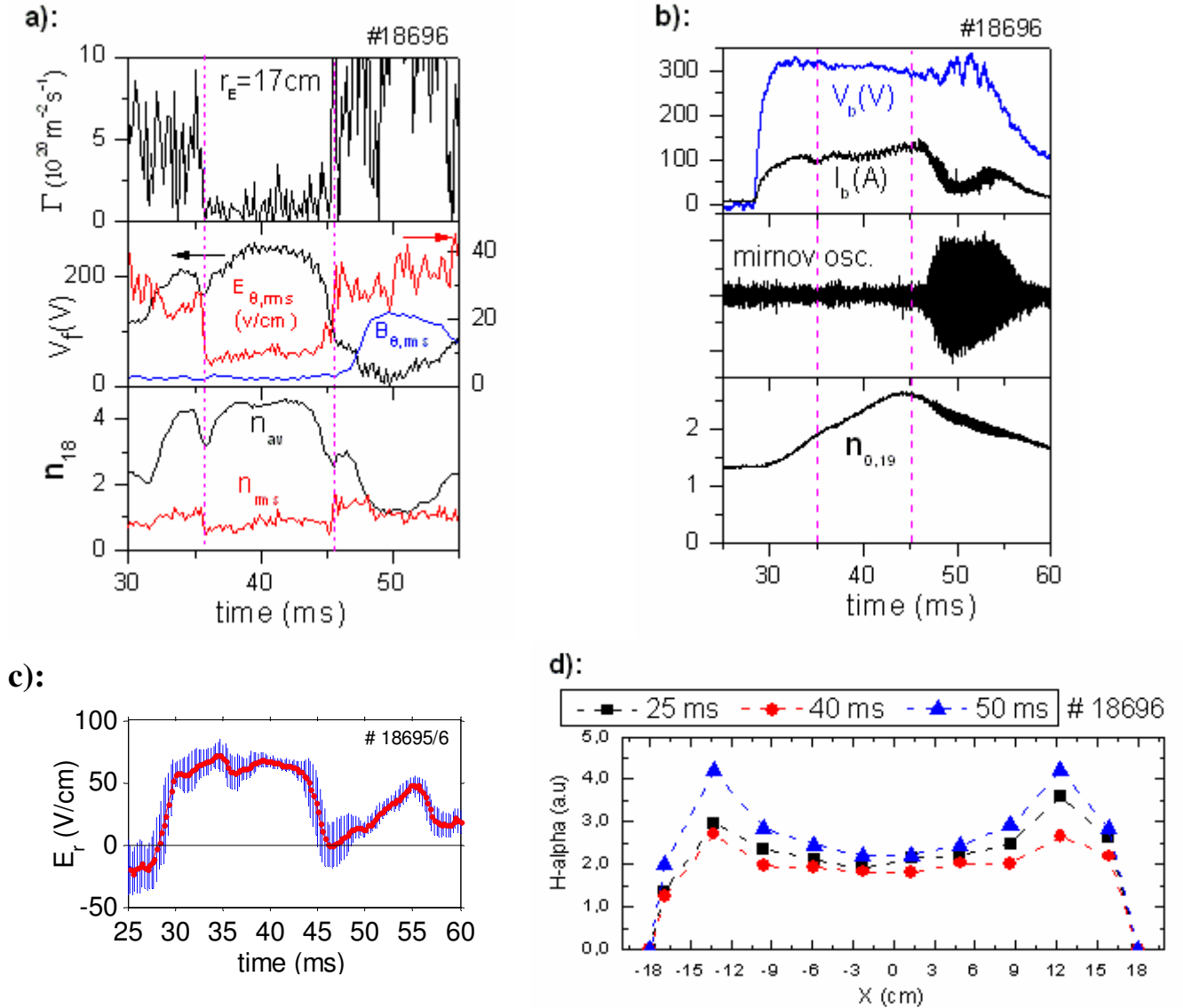


Figure 4. Effect of electrode voltage on edge plasma parameters. Plasma in regime II with electrode at  $r_E = 17.0$  cm, shot #18696. Temporal behaviour at  $r = 17.0$  cm of: (a) transport, floating potential, root mean square of the poloidal electric and magnetic field fluctuations  $E_{\theta,rms}$ ,  $B_{\theta,rms}$ , respectively; (b) voltage and electrode current, Mirnov oscillations, dB/dt, and central chord line-averaged current; (c) electric field at  $r = 18.0$  cm. (d) Radial profile of the  $H_\alpha$  emission at 28 ms before biasing, 41 ms and 42.5 ms with biasing and without and with MHD activity, respectively.

The plasma density grows gradually during the H mode which lasts for 10 ms, ending at 45 ms. Noticeable are the negative bumps on the floating potential, ion saturation current and on the electrode current just before the triggering of the H-mode. This did not perturb the

increase of the central chord density. Differently to the case of the shot #17694, here the onset of the MHD activity occurs at 47 ms, that is, 2 ms after the strong decrease of the radial electric field  $E_r$  at 45 ms. The average edge density begin to decrease already at about 2 ms before the end of the H mode, 4 ms before the rapid growth of the MHD activity. A bump of about 0.7 V<sub>peak</sub> (30%), in the loop voltage (not shown in the figure), occurs at 46 ms indicating cooling and, consequently, profile change and the MHD activity. On the other hand the fast decrease of the radial electric field is coincident with a burst of runaway electrons detected with a NaI scintillation crystal and photomultiplier. Therefore, it is possible that runaway electrons absorbing energy from the toroidal electron field, triggers the decrease of  $E_r$ , consequently destroying the transport barrier, i.e, in this case, the MHD activity is a consequence of the destruction of the barrier. The strong decay of the electrode current can be understood as an increase of the plasma resistivity. The loop voltage recovers after the MHD decay to the previous level. The spectrum of MHD modes is similar to the one shown in figure. 2(c) for shot # 18144 where the (3, 1) mode is dominant.

#### 4. Conclusion

The discharges of the tokamak TCABR were classified in two types, depending on the response to electrode biasing. Without application of voltage biasing the tokamak was tuned to obtain shots with weak or strong MHD activity, called regime I and II, respectively. Subsequent biasing resulted in strong excitation of MHD for regime I and partial or total suppression of MHD for regime II

In regime I the plasma enters the H mode but the barrier is destroyed at the onset of the MHD activity. The positive radial electric field decreases, recovering almost completely at the beginning of the MHD saturation. The degradation of the confinement can be explained by the plasma cooling caused by the radiation losses produced by impurities accumulated near the central region of the plasma, the excitation of MHD activity and the coupling of the dominant mode  $m = 2, n = 1$  with the  $m = 3, n = 1$ , overlapping the edge transport barrier, and producing strong changes in the electric field. This interpretation is in agreement with Stringer's neoclassical theory of impurity transport in the presence of electrostatic and magnetic fluctuations [5].

In regime II we have a more stable H mode which lasts for 10 ms, and is interrupted by the destruction of the transport barrier with a synchronized decrease of the radial electric field and increase of turbulence. However, the onset of the MHD activity occurs 2 ms later and it is a consequence of the barrier destruction. The cause of the effect on the barrier is, possibly, a short burst of high energy x-rays from runaway electrons absorbing energy from the toroidal electric field. After the destruction of the barrier the MHD activity is excited and appears in the loop voltage, and the increase in  $H_\alpha$  radial profile can be seen.

#### Acknowledgements

This work was supported by the FAPESP - Research Foundation for the Support of the Research of the State of Sao Paulo, CNPQ - National Council of Scientific and Technological Development, University of Sao Paulo, and IAEA-CRP-Joint Research Using Small Tokamaks

## References

- [1] F. Wagner *et al.* 1982 Phys. Rev. Lett **49** 1408
- [2] I. C. Nascimento *et al.* 2005 Nucl. Fusion **45** 796
- [3] L. G. Askinazi *et al.* 2006 Plasma Phys. Control. Fusion **48** A85
- [4] M. V. A. P. Heller *et al.* 2005 Czech. J. Phys. **55** 265
- [5] T. E. Stringer 1992 Nucl. Fusion **32** 1421